

## Slow Magnetosonic Solitons Detected by the Cluster Spacecraft

K. Stasiewicz,<sup>1</sup> P. K. Shukla,<sup>2</sup> G. Gustafsson,<sup>1</sup> S. Buchert,<sup>1</sup> B. Lavraud,<sup>3</sup> B. Thidé,<sup>1</sup> and Z. Klos<sup>4</sup>

<sup>1</sup>Swedish Institute of Space Physics, Box 537, SE-751 21 Uppsala, Sweden

<sup>2</sup>Institut für Theoretische Physik IV, Ruhr-Universität Bochum, D-44780 Bochum, Germany

<sup>3</sup>Centre d'Étude Spatiale des Rayonnements, Toulouse, France

<sup>4</sup>Space Research Centre, Polish Academy of Sciences, Warsaw, Poland

(Received 2 December 2002; published 27 February 2003)

Experimental evidence is provided for the existence of slow-mode magnetosonic solitons in the collisionless plasma at the magnetopause boundary layer. The solitons were detected by the fleet of Cluster spacecraft at the dusk flank of the magnetosphere as magnetic field depressions (up to 85%) accompanied with enhancement of the plasma density and temperature by a factor of 2. The solitons propagate 250 km/s with respect to the satellites and have perpendicular size of 1000–2000 km, which is a few ion inertial scale lengths. The comparison with numerical solutions of a theoretical model shows quantitative agreement between the model and observations.

DOI: 10.1103/PhysRevLett.90.085002

PACS numbers: 94.30.Di, 52.35.Sb, 52.35.Bj, 94.30.Tz

We present first observations of slow magnetosonic solitons detected in natural unbounded collisionless plasma by a fleet of four Cluster spacecraft [1]. Measurements were made at radial distance of  $18R_E$  at the magnetopause boundary layer, which is a current layer that separates the shocked and thermalized solar wind in the magnetosheath from the magnetic fields of the terrestrial origin. With multipoint measurements and complete plasma diagnostics of the Cluster mission we were able for the first time to provide all relevant parameters of the solitons and their environment.

On November 25, 2001, at 01-05 UT the Cluster satellites separated by  $\sim 2000$  km from each other were skimming the magnetopause layer moving close to a disturbed surface during a few hours. The magnetopause was strongly undulated by large amplitude surface waves induced by fast solar wind flow with velocity of 800 km/s. The solitary structures are seen inside the magnetosphere by the electric and magnetic field instruments as well as by most plasma detectors as short duration pulses ( $\sim 10$  s) which propagate with a speed of  $\sim 250$  km/s over slowly 1.3 km/s moving satellites. The position of Cluster satellites was  $(-4, 17, 5) R_E$  in geocentric solar ecliptic (GSE) coordinates. The structures seen in the magnetic field [2] represent depressions of  $-85\%$   $B_0$ , the ambient magnetic field, and propagate close to the perpendicular direction as deduced from the minimum variance analysis of the magnetic field. The shape of the structures is almost ideal  $-\text{sech}^2(x)$  as theoretically predicted by, e.g., the Korteweg-de Vries (KdV) equation [3,4]

In Fig. 1 we show one soliton seen by two spacecraft (C2, C4) with a relative time delay of 6 s which corresponds to a velocity 250 km/s, deduced from the known separation distance between the satellites. This soliton was not observed by the two other spacecraft located 2000 km closer to the Earth. The ambient plasma pa-

rameters at the locations of solitons were  $B_0 = 40$  nT, the plasma number density  $n_0 \approx 1 \text{ cm}^{-3}$ , the ion temperature  $T_i \approx 10^7$  K, and the electron temperature typically 8 times smaller than  $T_i$ . The  $\mathbf{E} \times \mathbf{B}$  flow velocity was 200–250 km/s. The ion detectors [5] show a comparable additional field-aligned flow component. Other derived plasma parameters are the Alfvén speed  $V_A = B/(\mu_0 n m_i)^{1/2} = 800$  km/s, the electron inertial length  $\lambda_e = c/\omega_{pe} = 5$  km, the ion inertial length  $\lambda_i = 200$  km, the ion gyroradius  $r_i = v_{ii}/\omega_{ci} = 100$  km, the plasma beta  $\beta = p/(B^2/2\mu_0) \approx 0.25$ , and the ion sound speed  $V_s \approx 400$  km/s. Here  $m_i$  is the ion mass,  $\omega_{pe}$  is

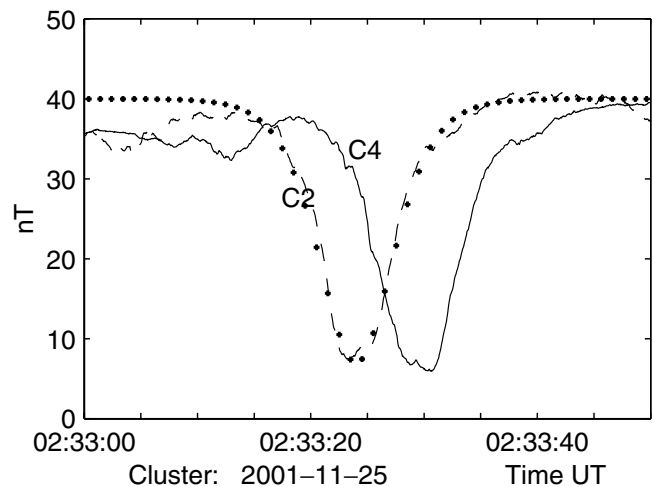


FIG. 1. A large scale soliton observed by Cluster spacecraft C2 (dashed) and C4 (solid) in the total magnetic field. Marked curve shows fit of  $b_0 \text{sech}^2[(t - t_0)/\delta t]$  with  $b_0 = -33$  nT and  $\delta t = 4.4$  s. The soliton moves with velocity  $u_0 \approx 250$  km/s and has a width of 2000 km. The position of Cluster satellites was  $(-4, 17, 5) R_E$  GSE.

the electron plasma frequency,  $\omega_{ci}$  is the ion cyclotron frequency, and  $c$  is the speed of light.

The solitons are observed inward from the magnetopause layer with tailward boundary layer flows (negative  $x$ -GSE direction). The adjacent flow in the magnetosheath is much higher and reaches 800 km/s. A large decrease of the magnetic field is accompanied by an increase of the plasma pressure through both the temperature (deduced from ion detector measurements) and the number density derived from the satellite potential (shown in Fig. 2). Inside the solitons the plasma density is increased by a factor of 2. Similar densities are derived from the moments of ion distribution function. The ion species at the boundary layer are predominantly protons. The soliton velocity in respect to the background medium cannot be completely determined because it is observed only by two spacecraft. From projections of the velocity vectors onto the interspacecraft position vector, we estimate the soliton speed relative to the medium as  $\sim 80$  km/s, which is much smaller than the local Alfvén speed (800 km/s), and, therefore, the solitary wave could correspond to the slow magnetosonic mode.

Magnetic holes, depressions in the magnetic field magnitude associated with enhancements in density and kinetic pressure, have been observed previously inside the magnetosphere [6,7], at the magnetopause [8], in the solar wind, and in the interplanetary medium [9,10]. Most researchers have interpreted magnetic holes as related to nonpropagating mirror mode waves generated in a high-beta plasma by anisotropic ion distributions. Relation of magnetic holes to solitons was suggested in Ref. [11] and to tearing mode reconnection structures at the magnetopause in [12].

Nonlinear waves and solitons in collisionless plasmas have been investigated within the framework of two-fluid equations of magnetohydrodynamics as well as with

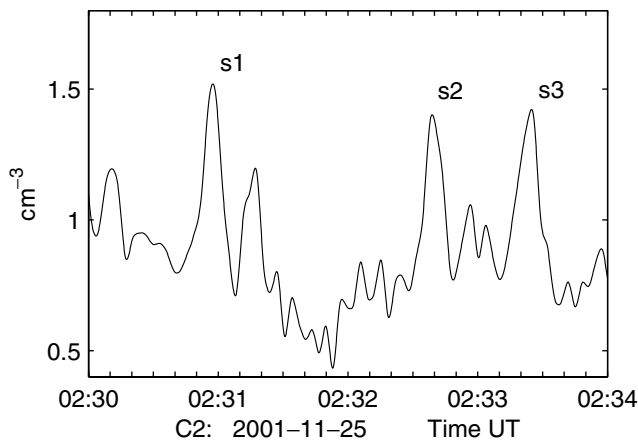


FIG. 2. Density enhancements ( $s1$ ,  $s2$ ,  $s3$ ) that correspond to three solitons associated with deep magnetic holes similar to that in Fig. 1. Peak labeled  $s3$  corresponds to soliton C2 in Fig. 1.

kinetic plasma theory. The natural wave modes at frequencies below the ion gyrofrequency consist of the Alfvén wave and two magnetosonic, slow and fast, modes. For propagation at sufficiently large angles to a uniform magnetic field, it was shown using reductive perturbation theory that nonlinear dispersive fast and slow MHD waves obey the KdV equation [13,14]. The dispersion of magnetosonic waves comes from the ion perpendicular inertia caused by the finite frequency effect (the Hall effect in the generalized MHD description), while nonlinearities arise due to the ion advection and divergence of the nonlinear ion flux, as well as from the nonlinear Lorentz forces acting on the electron and ion fluids. On the other hand, for quasiparallel propagation the dynamics of modulated (by zero-frequency electrostatic perturbations) Alfvén wave packets is governed by the derivative nonlinear Schrödinger equation (DNSE) [11,15,16]. However, both the KdV equation and the DNSE describe the dynamics of finite (but small) amplitude nonenvelope and envelope solitons.

Recently, a fully nonlinear treatment of two-fluid equations with thermal effects of ions and electrons has been presented by McKenzie and Doyle [17]. We shall follow this approach and introduce plane geometry with all variables depending on the  $x$  coordinate, which is also the wave propagation direction. The ambient magnetic field  $B_0(\cos\alpha, 0, \sin\alpha)$  has angle  $\alpha$  with the  $x$  axis ( $B_x = \text{const}$ ). In the wave frame of reference, we have initial incoming flow speed  $u_0$  and the magnetic field  $B_0 = (B_{x0}^2 + B_{z0}^2)^{1/2}$ . In such a one-dimensional geometry we are seeking wave solutions in the form  $\Phi(x - ut)$ . The fluid equations can be conveniently expressed as momentum and energy density flux conservation. Let us assume the polytropic equation for pressure

$$p_e + p_i = p_0 u^{-\gamma}. \quad (1)$$

In the wave frame, the  $x$  component of momentum flux density takes the form

$$nm_i u_x^2 + p + B^2/2\mu_0 = \text{const}. \quad (2)$$

We introduce the normalized quantities

$$u = u_x/u_0, \quad b = B/B_0, \quad (3)$$

and the Mach numbers

$$M_s = \frac{u_0}{V_s}, \quad M_A = \frac{u_0}{V_A}, \quad (4)$$

where  $V_s = \sqrt{\gamma p_0/n_0 m_i}$  is the ion sound speed. Using the above definitions, we can express (2) in dimensionless form as

$$P(u) = u - 1 + \frac{u^{-\gamma} - 1}{\gamma M_s^2} = \frac{(1 - b^2)}{2M_A^2}. \quad (5)$$

Please note that the continuity equation implies  $n/n_0 = u^{-1}$ . Thus, Eq. (5) describes a general dependence of

the density and magnetic field variation for arbitrary, one-dimensional structures, provided that Eq. (1) is applicable. Equation for the plasma flow can be expressed as [17]

$$u \left( 1 - \frac{1}{M_s^2 u^{\gamma+1}} \right) \frac{du}{dx} = \pm \frac{M_{\parallel}}{\lambda_i} \left[ \frac{-2M_{\parallel}^2(P+U)}{M_{\perp}^2(M_{\parallel}^2-1)} - \frac{(P+M_{\parallel}^2U)^2}{(M_{\parallel}^2-1)^2} \right]^{1/2}, \quad (6)$$

where  $\lambda_i = V_A/\omega_{ci}$ ,  $M_{\parallel} = M_A/\cos\alpha$ ,  $M_{\perp} = M_A/\sin\alpha$ , the plasma momentum  $P$  is given by (5) and the normalized energy flux  $U$  is given by

$$U(u) = \frac{1}{2}(1-u^2) + \frac{1-u^{-(\gamma-1)}}{M_s^2(\gamma-1)}. \quad (7)$$

No approximations have been made in deriving Eqs. (5)–(7) from the two-fluid superset. Linearizing (6),  $u = 1 + u_1$ , and seeking solutions in the form  $u_1 \propto \exp(kx)$ , we find a dispersion relation

$$k^2 = \frac{M_{\parallel}^2}{\lambda_i^2} \left[ \frac{1}{M_{\perp}^2(1-M_{\parallel}^{-2})(1-M_s^{-2})} - 1 \right]. \quad (8)$$

A necessary condition for solitary waves is  $k^2 > 0$ , which implies

$$m \equiv \frac{\sin^2\alpha}{(M_A^2 - \cos^2\alpha)(M_s^2 - 1)} > 1. \quad (9)$$

Solitary waves exist for certain propagation angles and Mach numbers prescribed by (9). We have solved numerically the nonlinear Eq. (6) for the slow-mode branch of magnetosonic solitons, which can give the observed anticorrelation between the density enhancement and magnetic field depression given by (5). In Fig. 3 we show numerical solutions for the variations of the density  $n = u^{-1}$  and the magnetic field  $b$ . The density is compressed by a factor of 2.3 and the magnetic field depressed by  $\sim 80\%$ , which are in excellent agreement with experimental data shown in Figs. 1 and 2. For given plasma parameters  $M_A$ ,  $M_s$ , Eq. (9) determines the range of  $\alpha$  where balance between dispersion and nonlinearity permits solitary wave solutions. In this particular case, slow magnetosonic solitons are possible within the propagation angles  $\alpha \approx 82^\circ$ – $84^\circ$ . In the lower range of  $\alpha$ , solitons become smaller and wider. The ion sound speed is determined from measurements of the plasma pressure, which gives  $\beta \approx 0.25$  in the background plasma, and thus  $V_s/V_A \approx \beta^{1/2} \approx 0.5$ . We should also point out that observations show that the slow-mode magnetosonic solitons are stable and do not exhibit appreciable variations during the observations separated 6 s ( $f_{ci} \approx 0.6 \text{ s}^{-1}$ ) in time, or 2000 km in space. The electron Landau damping rate,  $\gamma_{\pm}$ , of linear (slow/fast) magnetosonic waves at the

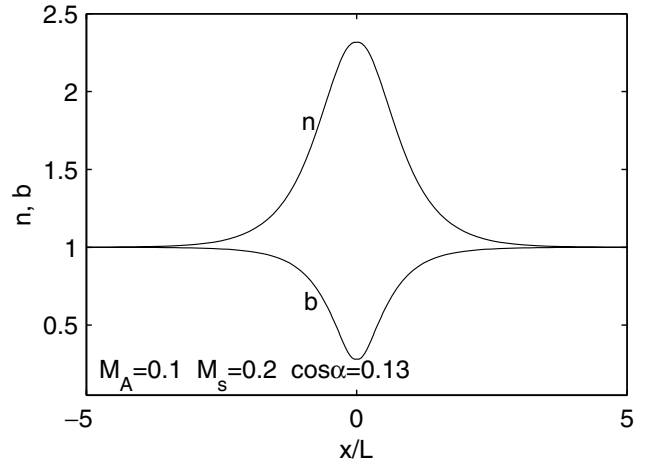


FIG. 3. Numerical solutions of the nonlinear two-fluid equations for the plasma density  $n$ , and the magnetic field  $b$ , which give solitary structures that resemble observations. The adopted parameters are  $u_0 = 80 \text{ km/s}$ ,  $V_A = 800 \text{ km/s}$ ,  $V_s/V_A = 0.5$ ,  $\gamma = 5/3$ , and  $\alpha = 83^\circ$ . The unit length is  $\lambda_i = V_A/\omega_{ci}$ .

magnetopause boundary layers is insignificant since  $\gamma_{\pm}/\omega \sim \sqrt{m_e/m_i}$  for  $V_s \sim V_A$  [18]. The structures are also repetitive, and several solitons observed during a 20 min period attained similar amplitude and width in an apparently similar plasma environment.

In conclusion, we have presented the evidence of non-envelope magnetosonic solitons which are detected by the Cluster spacecraft at the magnetopause boundary layer. The magnetosonic solitons are characterized by magnetic field depressions (up to 85%) accompanied by a local increase of plasma density and temperature, over the spatial scale of 2000 km. We have carried out a numerical analysis of the fully nonlinear two-fluid MHD model and have shown that the magnetic field and density profiles of finite amplitude magnetosonic solitons are in good agreement with observations. Thus, the magnetopause boundary layer turns out to be a unique laboratory for testing the theory of magnetosonic solitary waves and the applicability of fluid equations to collisionless plasma.

This research was partially supported by the European Commission (Brussels) through Contract No. HPRN-CT-2001-00314 for carrying out the task of the research training network entitled “Turbulent Boundary Layers in Geospace Plasmas.”

- 
- [1] C. P. Escoubet, M. Fehringier, and M. Goldstein, *Ann. Geophys.* **19**, 1197 (2001).
  - [2] A. Balogh *et al.*, *Ann. Geophys.* **19**, 1207 (2001).
  - [3] V. I. Karpman, *Non-linear Waves in Dispersive Media* (Pergamon Press, New York, 1975).

- [4] E. Infeld and G. Rowlands, *Nonlinear Waves, Solitons and Chaos* (Cambridge University Press, Cambridge, U.K., 2000).
- [5] H. Réme *et al.*, *Ann. Geophys.* **19**, 1303 (2001).
- [6] H. Lühr and N. Klöcker, *Geophys. Res. Lett.* **14**, 186 (1987).
- [7] R. Treumann, L. Brostrom, J. LaBelle, and N. Scopke, *J. Geophys. Res.* **95**, 19 099 (1990).
- [8] J. M. Turner, L. F. Burlaga, N. F. Ness, and J. F. Lemaire, *J. Geophys. Res.* **82**, 1921 (1977).
- [9] D. Winterhalter, M. Neugebauer, B. E. Goldstein, E. J. Smith, S. J. Bame, and A. Balogh, *J. Geophys. Res.* **99**, 23 371 (1994).
- [10] B. T. Tsurutani and C. M. Ho, *Rev. Geophys.* **37**, 517 (1999).
- [11] K. Baumgärtel, *J. Geophys. Res.* **104**, 28 295 (1999).
- [12] K. Stasiewicz, C. Seyler, F. Mozer, G. Gustafsson, J. Pickett, and B. Popielawska, *J. Geophys. Res.* **106**, 29 503 (2001).
- [13] T. Kawahara, *J. Phys. Soc. Jpn.* **27**, 1331 (1969).
- [14] Y. Ohsawa, *Phys. Fluids* **29**, 1844 (1986).
- [15] A. Rogister, *Phys. Fluids* **14**, 2733 (1971).
- [16] C. F. Kennel, B. Buti, T. Hada, and R. Pellat, *Phys. Fluids* **31**, 1949 (1988).
- [17] J. F. McKenzie and T. B. Doyle, *Phys. Plasmas* **9**, 55 (2002).
- [18] A. I. Akhiezer *et al.*, *Plasma Electrodynamics, Linear Theory Vol. 1* (Pergamon Press, New York, 1975), p. 259.